수의학석사 학위논문

Adipose Tissue Inflammation in Weight Cycling Mice

중량 사이클링에 의한 마우스 지방 조직 염증에 관한 연구

2016년 8월

서울대학교 대학원
수의학과 수의생명과학 전공
성 혜 림

수의학석사 학위논문

Adipose Tissue Inflammation in Weight Cycling Mice

중량 사이클링에 의한 마우스 지방 조직 염증에 관한 연구

2016년 8월

서울대학교 대학원
수의학과 수의생명과학 전공
성 혜 림

Adipose Tissue Inflammation in Weight Cycling Mice

지도교수 성 제 경

이 논문을 수의학석사 학위논문으로 제출함

2016년 4월

서울대학교 대학원

수의학과 수의생명과학 전공

성 혜 림

성혜림의 수의학석사 학위논문을 인준함

2016년 6월

위 원 장 윤 여 성 (인)

부 위 원 장 성 제 경 (인)

위 원 이 윤 희 (인)

Abstract

Adipose Tissue Inflammation in Weight Cycling Mice

Hyerim Sung
Department of Veterinary Biomedical Sciences
The Graduate School
Seoul National University

Obesity correlates with the development of metabolic diseases, and weight loss is the ideal approach to ameliorate obesity. However, weight loss is rarely maintained, leading to weight regain. This phenomenon, termed 'weight cycling', is also known as 'yo-yo dieting'. Weight cycling increases the risk of morbidity and mortality in both humans and mice, although the mechanisms that regulate weight cycling are not well understood. We subjected mice to a diet-switch protocol, designed to induce weight cycling, to determine the differences between mice that undergo weight cycling and mice that experience weight gain without weight cycling. Weight cycling produced aggravated metabolic phenotypes including increased body weight and dyslipidemia. Weight cycling produced severe adipose tissue inflammation, including hypertrophic adipocytes, and an increased

number of crown-like structures. Upon weight cycling, invasive immune cells in adipose tissue entered a pro-inflammatory state. Therefore, the metabolic phenotype was much severely aggravated, and adipose inflammation was significantly increased, in the weight cycling group compared to the weight gain group. In addition, the expression of multiple immune-related genes and pro-inflammatory cytokine genes was elevated in the weight cycling group, compared to the weight gain group. These studies indicate that altered immune cell populations and gene expression patterns in adipose tissue may contribute to metabolic aggravation during weight cycling.

Keywords : Obesity, Weight cycling, Mice, Adipose tissue, Inflammation.

Student Number : 2013-23443

Contents

List of Tables

List of Figures

List of abbreviations

ARG1	Arginase 1
C1qc	Complement component 1, Q subcomponent, C Chain
CD11b	Cluster of differentiation molecule 11B
CD11c	Complement component 3 receptor 4 subunit
CD206	C-type 1 lectin receptor
CD3	Cluster of differentiation 3
CD3g	CD3g molecule, Gamma
CD4	Cluster of differentiation 4
CD45	Lymphocyte common antigen
CD64	Cluster of differentiation 64
CD8	Cluster of differentiation 8
CLS	Crown like structure
EDTA	Ethylenediaminetetraacetic acid
eWAT	Epididymal white adipose tissue
F4/80	EGF-like module-containing mucin-like hormone receptor-like 1
FACS	Fluorescence-activated cell sorting
Foxp3	Forkhead box P3
Gbp2	Interferon-induced guanylate-binding protein 2
H&E	Hematoxylin and eosin
H2-Aa	Histocompatibility 2, class II antigen A, alpha
H2-DMb1	Histocompatibility 2, class II, locus Mb1
HRP	Horseradish peroxidase
I-A/I-E	MHC class II-associated invariant chain

IFNγ	Interferon gamma
IL10	Interleukin 10
IL4	Interleukin 4
IL6	Interleukin 6
Irgm2	Immunity-related GTPase family M member 2
Itgax	Complement component 3 receptor 4 subunit
MCP1	Monocyte chemotactic protein 1
Mgl1	Macrophage galactose-type C-type lectin 1
Nkg7	Natural killer cell granule protein 7
NOS2	Nitric oxide synthase 2
PBS	Phosphate-buffered saline
Siglec-F	Sialic acid-binding immunoglobulin-like lectin F
SVF	Stromal vascular fraction
TBS	Tris-buffered saline
TDW	Three-distilled water
TNF-α	Tumor necrosis factor alpha
Treg	Regulatory t cell
Ym1	Beta-N-acetylhexosaminidase

Ⅰ. Introduction

Obesity is related to type 2 diabetes, cardiovascular disease, and certain forms of cancer (P, K., 2007). In particular, obesity-induced chronic inflammation is a key component in the pathogenesis of insulin resistance and the metabolic syndrome (de Luca C & JM, 2008). Insulin resistance in the setting of obesity results from a combination of altered functions in insulin target organs and from the accumulation of macrophages that secrete pro-inflammatory mediators (Olefsky & Glass, 2010). Furthermore, obesity-induced insulin resistance in adipose tissue is promoted by a transition in macrophage polarization from an alternative M2 activation state to a classical M1 activation state (Weisberg *et al*, 2003; Xu *et al*., 2003; Lumeng, Bodzin, & Saltiel, 2007). In addition to innate immune cell activation in obesity (Lumeng, 2013), adaptive immune cells are involved in adipose tissue inflammation during obesity. Obesity, induced by feeding a high fat diet, is associated with a decrease in $CD4^+$ regulatory T cells and T helper 2 cells (Cipolletta, Kolodin, Benoist, & Mathis, 2011; Winer *et al*., 2011). Moreover, obesity promotes the entry of B cells, $CD4^+$ T helper 1 cells and $CD8^+$ cytotoxic T cells into adipose tissue (Winer *et al*., 2009; Strissel *et al*., 2010; Nishimura *et al*., 2009). Both innate and adaptive immunity contribute to regulate obesity-induced inflammation (Schipper HS, Prakken B, Kalkhoven E & M, 2012).

Whereas weight loss is the ideal approach to counteract the obesity, it is rarely maintained (Rena R Wing & Hill, 2001). Furthermore, after losing weight, up to 80% of people regain a

significant portion of the lost weight within one year (Rena R Wing & Hill, 2001; Kraschnewski *et al.*, 2010; Weiss, Galuska, Kettel Khan, Gillespie, & Serdula, 2007). This phenomenon, termed 'weight cycling', is also known as 'yo-yo dieting', and it is characterized by repeated bouts of weight loss and regain (Blackburn GL et al., 1989). Weight loss decreases the number of macrophages within adipose tissue, reduces inflammation, and improves insulin sensitivity (Li *et al.*, 2010; Kosteli *et al.*, 2010; Rector *et al.*, 2007). On the other hand, weight cycling promotes fat gain, enhances adipose tissue inflammation, and impairs systemic glucose tolerance (Dankel SN *et al.*, 2014; Barbosa-da-Silva S, Fraulob-Aquino JC, Lopes JR, Mandarim-de-Lacerda CA & MB., 2012; Anderson EK, Gutierrez DA, Kennedy A & AH., 2013). Moreover, weight cycling increase the risk of morbidity and mortality, both in humans and rodents (Mehta, Smith, Muhammad, & Casazza, 2014).

While the detrimental effect of weight cycling is recognized, the cause of the metabolic dysfunction associated with weight cycling remains unknown. Therefore, we subjected mice to a diet-switch protocol, designed to induce obesity by weight cycling, and determined the differences in metabolic phenotype between the weight cycling group and the group that experience weight gain without cycling. The current study consists of three periods in which mice are fed diets to promote weight gain, weight loss, and weight regain. In the first period, mice were fed a high fat diet to induce obesity. In the second period, their diet was switched to chow to promote weight loss, until a similar weight to the control group was achieved. In the final period, mice were fed a high fat diet again to promote weight regain. Mice in the

weight cycling group had a more severe obesity-related phenotype, as assessed using body weight, liver and adipose tissue weight, and blood metabolic parameters. In addition, enhanced hepatic steatosis—elevated accumulation of lipids in the liver—was observed in the weight cycling group. Mice in the weight cycling group had increased adipose tissue inflammation, including increased hypertrophic adipocytes, crown-like structure number, and pro-inflammatory immune cells within adipose tissue. Consequently, expression of multiple immune-related genes, including pro-inflammatory cytokine genes, were increased in the adipose tissues of the weight cycling group compared to weight gain group. Therefore, alterations of immune cell populations and their gene expression profiles within adipose tissue may contribute to the aggravated metabolic phenotype that occurs during weight cycling.

Ⅱ. Materials and Methods

1. Experimental design and laboratory animals

4-week-old male C57BL6/N mice were purchased from Central Lab. Animal Inc. (Seoul, Republic of Korea). The animals were housed at 24 ± 2℃ with a 12 h light/dark cycle. They were fed a chow diet (NIH-31, Ziegler Bros., Inc., PA, USA) *ad libitum*, along with tap water. After 1 week of acclimatization, each mouse was randomly assigned to one of four groups, according to its weight measurement. For a total experimental period of 16 weeks, the mice in the weight cycling group were fed a high fat diet (60% kcal% fat, #D12492, Research Diets, NJ, USA) for 8 weeks. Following this, their diet was changed to a chow diet for 4 weeks, and then changed to a high fat diet for a further 4 weeks. The mice in the weight gain group were fed a chow diet for 12 weeks, and had their diet changed to a high fat diet for 4 weeks. The mice in the weight maintenance group were fed a high fat diet for 8 weeks, and had their diet changed to a chow diet for 8 weeks. The mice in the control group were fed a chow diet for 16 weeks.

A summary of the diet feeding protocol is presented at Table 1. Nutritional information pertaining to the chow diet and the high fat diet is arranged in Table 2 and Table 3.

All mice had their body weights measured weekly. This experimental protocol was carried out according to the "Guide for Animal Experiments" (edited by Korean Academy of Medical Sciences), and was approved by the Institutional Animal Care and Use Committee (IACUC) of Seoul National University

(Approval number: SNU-140205-2-1).

Table 1. Diet feeding protocol for weight cycling

Groups[1)]	Diet feeding scheme		
	8weeks	4weeks	4weeks
Control	Chow diet	Chow diet	Chow diet
Weight Cycling	High fat diet	Chow diet	High fat diet
Weight Gain	Chow diet	Chow diet	High fat diet
Weight Maintenance	High fat diet	Chow diet	Chow diet

[1)] Male C57BL/6N mice were placed on a chow diet or high fat diet for 8-4-4 weeks intervals

Table 2. Composition of the chow diet

	NIH-31 (Chow diet)
	(%)
Protein	18
Carbohydrate	4.5
Fat	5.3
Gross Energy (Kcal/gm)	3.97
Ingredients	**(%)**
Ground No. 2 Yellow Corn	21
Ground Whole Wheat	35.37
Wheat Middlings	10
Fish Meal (60%)	9
Soybean Meal (47.5%)	5
Soybean Oil	1
Alfalfa Meal (17%)	2
Corn Gluten Meal (60%)	2
Brewers Dried Yeast	1
Dicalcium Phosphate	1.5
Limestone	1.5
Salt	0.5
Premixes	0.63

(Information provided from Ziegler Bros., Inc. PA, USA)

Table 3. Composition of the high fat diet

	D12492 (High fat diet)	
	(g%)	(kcal%)
Protein	26	20
Carbohydrate	26	20
Fat	35	60
Gross energy (kcal/gm)	5.24	
Ingredients	(g)	(kcal)
Casein, 80 Mesh	200	800
L-systine	3	12
Corn Starch	0	0
Maltodextrin 10	125	500
Sucrose	68.8	275
Cellulose, BW200	50	0
Soybean Oil	25	225
Lard	245	2205
Mineral Mix S10026	10	0
Dicalcium Phosphate	13	0
Calcium Carbonate	5.5	0
Potassium Citrate	16.5	0
Vitamin Mix V10001	10	40
Choline Bitartate	2	0

(Information provided from Research Diets, Inc. NJ, USA)

2. Blood chemistry

Blood glucose and total cholesterol were measured in 20 μL serum samples by a Hitachi 7180 biochemistry auto analyzer (Hitachi Ltd., Tokyo, Japan). A 'Triglyceride Quantification Colorimetric/Fluorometric Kit' (K622-100, Biovision, CA, USA) was used, according to the manufacturer's instructions, for the quantitative determination of hepatic triglyceride accumulation in the liver.

3. Histopathology

To obtain representative samples of liver and epididymal adipose tissue, samples were taken at the end of the experiments. Each organ was weighed and fixed with 4% paraformaldehyde (BIOSESANG, Republic of Korea) overnight at room temperature. The fixed tissue samples were dehydrated, cleared, and embedded in paraffin. A 4 μm section was taken from each of the embedded tissue pieces and stained with hematoxylin and eosin, according to a standard procedure. For staining with, liver tissue was cryoprotected by infiltration with 30% sucrose. The liver tissue sample was cut using a cryostat (Leica, Germany). The liver samples were washed with TDW for 5 minutes, then washed once with 50% isopropyl alcohol, and then stained with Oil Red O solution (6 parts of 0.5% Oil Red O powder in isopropanol and 4 parts of water) for 20 minutes at 54℃ in a dry oven. The samples were then rinsed with tap water and counter stained with hematoxylin. Tissue sections were analyzed under a microscope (Olympus Co. Japan) equipped with a digital camera (DP71, Olympus). Images were captured (4 - 5 per section) from

several stained pieces of adipose tissue from each mouse. There were 4 mice per group, yielding a total of 15 - 20 images per experimental group. Adipocyte size was quantified from each image using *ImageJ* software (National Institutes of Health, Bethesda, MD, USA).

4. Immunohistochemistry

For immunohistochemical staining of epididymal adipose tissue, deparaffinized sections were heated for 20 minutes in a pressure cooker containing antigen retrieval buffer (AR-6544, IBCS, WA, USA). Sections were treated for 15 minutes with 3% H_2O_2 in 0.1 M Tris-buffered saline (TBS, pH7.4), to quench endogenous peroxidases. For endogenous enzyme blocking, the sections were treated with normal goat serum (S-1000, Vector, CA, USA) in 0.01 M TBS using F4/80 (1:100, sc-59171, Santa Cruz Biotechnology, CA, USA), CD11c (1:100, ab33483, Abcam, UK) as primary antibody for overnight in 4℃. Sections were incubated with EnVision/HRP anti-rabbit/mouse (K-5007, DAKO, CA, USA) for 30 minutes. Peroxidase bound to the antibody complex was visualized by treatment with 3,3′-diaminobenzidine chromogen substrate solution (K-5007, DAKO, CA, USA). Sections were examined by bright-field microscopy.

5. Isolation of the stromal vascular fraction and FACS analysis

Mice were sacrificed and immediately perfused with 30 mL PBS. The epididymal adipose tissue was finely chopped with scissors following its extraction. A 2 mL collagenase sample (C6885,

Sigma Aldrich, MO, USA) was added to the minced adipose tissue and incubated for 8 minutes at 37℃ with shaking. At the end of the incubation, 0.5 M EDTA (CMS005, Cosmo Genetech, Republic of Korea) was added to the cell suspension, with gentle stirring. The cell suspension was filtered through a 70 μm filter (93070, SPL, Republic of Korea) and centrifuged at 1400 $\times g$ for 10 minutes. The top layer of adipocytes was removed, and the SVF pellet was washed twice with FACS buffer (PBS with 2% fetal bovine serum). The cell suspension was then centrifuged at 1400 $\times g$ for a further 10 minutes, resuspended with 200 μL 1X RBC lysis buffer (00-4300-54, eBioscience, CA, USA : 1X from 100X buffer using distilled water). After 2 minutes, the cells were washed twice with FACS buffer. Isolated stromal vascular cells were first incubated with Fc block (93, BioLegend, CA, USA) for 15 minutes at room temperature. Once washed with FACS buffer, cells were incubated with both a labeled monoclonal antibody and an isotype control. The labeled monoclonal antibodies were directed against: CD206 (MMR) (C068C2, BioLegend), CD64 (FcγRI) (X54-5/7.1, BioLegend), CD45 (30-F11, BioLegend), CD11c (N418, BioLegend), CD11b (M1/70, BioLegend), I-A/I-E (MHC II) (M5/114.15.2, BioLegend), F4/80 (A3-1, Serotec, NC, USA), NK1.1 (PK136, BioLegend), Siglec-F (E50-2440, BD Horizon, CA, USA), CD4 (GK1.5, BD Pharmingen, CA, USA), Foxp3 (FJK-16s, eBioscience), CD19 (6D5, BioLegend), CD3 (17A2, BioLegend). Samples were analyzed by flow cytometry using a FACS Canto II system (BD Biosciences, San Jose, CA, USA), and *FlowJo* software (Tree Star, Inc., Ashland, OR, USA). The gating strategy used for analysis is explained in Figure 1.

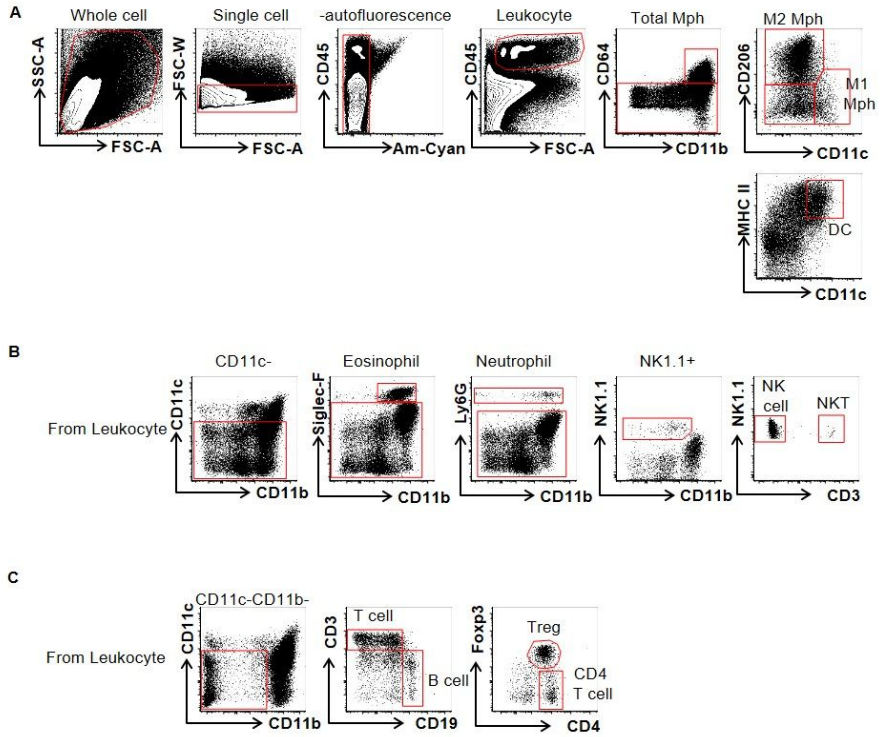

Figure 1. Gating strategy for FACS analysis.

Epididymal adipose tissue samples were dissected, and separated into adipocyte and stromal vascular fractions. (A) Gating strategy for the macrophage subpopulation based on forward and side scatter. Doublets and auto-fluorescent cells were excluded. Leukocytes were selected, then stained with antibodies directed against CD45, CD64, CD206, CD11c, and MHC II. (B) Gating strategy for the granulocyte subpopulation based on forward and side scatter. Leukocytes were isolated using the gating strategy described in panel (A), and then stained antibodies directed against CD11c, CD11b, Siglec-F, Ly6C, NK1.1 and CD3. (C) Gating strategy for the T cell subpopulation. Leukocytes were

isolated using the gating strategy described in panel (A), and then stained antibodies directed against CD11c, CD11b, CD3, CD19, Foxp3, and CD4.

6. RNA isolation, cDNA synthesis, and real-time RT-PCR

Total RNA was extracted from epididymal fat tissue using a 'PureLink RNA Mini Kit' (Invitrogen, CA, USA). The RNA was quantified using a NanoVue spectrophotometer (GE Healthcare, NJ, USA). cDNA was synthesized using an AccuPower CycleScript RT PreMix (K-2044, Bioneer, Republic of Korea), according to manufacturer's protocol. Quantitative real-time PCR was performed with SYBR Green dye using a 7500 Real Time PCR System (Applied Biosystems, UK). All gene expression profiles were normalized to the control gene, 36B4, and presented as expression relative to control group. The sequences of the primers used for real-time quantitative PCR are provided in Table 4.

Table 4. Sequence of primers used for real-time quantitative PCR

Gene	Sequence
F4/80	CTTTGGCTATGGGCTTCCAGTC
	GCAAGGAGGACAGAGTTTATCGTG
MCP1	CTTCTGGGCCTGCTGTTCA
	CCAGCCTACTCATTGGGATCA
NOS2	CCAAGCCCTCACCTACTTCC
	CTCTGAGGGCTGACACAAGG
Mgl1	TGAGAAAGGCTTTAAGAACTGGG
	GACCACCTGTAGTGATGTGGG
Ym1	AGAAGGGAGTTTCAAACCTGGT
	GTCTTGCTCATGTGTGTAAGTGA
ARG1	CTCCAAGCCAAAGTCCTTAGAG
	AGGAGCTGTCATTAGGGACATC
Itgax	CTGGATAGCCTTTCTTCTGCTG
	GCACACTGTGTCCGAACTC
CD4	TCTGGCAACCTGACTCTGAC
	TCATCACCACCAGGTTCACT
CD19	CTGTATGGTTTCTCTGGTGGCTTT
	CTGTATGGTTTCTCTGGTGGCTTT
Foxp3	CCCATCCCCAGGAGTCTTG
	ACCATGACTAGGGGCACTGTA
IFNγ	GCTCTTACTGACTGGCATGAG
	CGCAGCTCTAGGAGCATGTG
TNF-α	ACGGCATGGATCTCAAAGAC
	AGATAGCAAATCGGCTGACG

IL6	TAGTCCTTCCTACCCCAATTTCC
	TTGGTCCTTAGCCACTCCTTC
IL10	GCTCTTACTGACTGGCATGAG
	CGCAGCTCTAGGAGCATGTG
IL4	CCCCAGCTAGTTGTCATCCTG
	CGCATCCGTGGATATGGCTC
Adiponectin	GAATCATTATGACGGCAGCA
	TCATGTACACCGTGATGTGGTA
Irgm2	GATCTCGGATCCGGGTAACGCGAT
	TAACAGAACTTCCTTGGCTTTGGCAGCAG
Nkg7	AGCCAAGAGACTCAAGTAGCAGGT
	TGGGATGCAAGACAGAACCAGGAA
C1qc	AGGGCCGATACAAACAGA
	CCGATGGATCAGGAACCA
Gbp2	GAAAAGCTGCTTCTTCTTCTTCTCT
	TCAAGACATGTTGTCACAGTGG
H2-DMb1	TGCTGGTCCTCAGTCT
	GGAAACACAGTATGTGAAGTC
H2-Aa	AGCTCACAATCCACCAAACC
	TGGCCTATAGAACAGGCAGC
CD3g	TGGAGAAGCAAAGAGACTGACA
	GCCATCCACTTGTACCAAATTC
36B4	GAGGAATCAGATGAGGATATGGGA
	AAGCAGGCTGACTTGGTTGC

7. Statistical analyses

Results were expressed as the mean ± SEM. *SPSS* (version 14.0, IBM, NY, USA) was used for all statistical analyses. Data were analyzed using a one-way ANOVA, and followed by a *post hoc* Student's *t*-test provided the ANOVA was significant. A two-way ANOVA was used to compare measurements with two different variables. A p-value <0.05 was considered statistically significant.

Ⅲ. Results

1. Obesity-related phenotype in mice subjected to weight cycling

To investigate the phenotypic differences produced by weight cycling, four groups of mice were designed (Figure 2A). The study consisted of three periods in which mice were fed diets to either gain weight, lose weight, or regain weight. Mice were randomly assigned to four groups: 1) A control group that received a chow diet continuously for the duration of the study; 2) The weight cycling group, placed on a high fat diet for 8 weeks to induce obesity, then switched to a chow diet for 4 weeks to promote weight loss, and then placed back on a high fat diet 4 weeks to induce subsequent obesity; 3) The weight gain group, which was maintained on a chow diet for 12 weeks, and then switched to a high fat diet for 4 weeks; 4) The weight maintenance group, which was switched from a high fat diet to a chow diet after 8 weeks, maintaining the chow diet for the remaining 8 weeks of the study. After the mice in the weight cycling group were switched over to a chow diet, their weight normalized to the mean body weight of the control mice within 4 weeks. The mice were fed a high fat diet for 4 weeks during the weight regain period. The mean body weight for each group was measured (Figure 2B). When placed on a high fat diet, the mice gained weight dramatically. After the mice were switched to a chow diet, their weight normalized to the body weight of control mice. Subsequent to being fed a high fat diet, the weight cycling group experienced significant weight gain compared to the weight

gain group ($p<0.05$). Similarly, the weight cycling group had an increased liver weight compared to the weight gain group (Figure 3A). In addition, the epididymal white adipose tissue weight was increased in both the weight cycling and the weight gain groups (Figure 3B). Total fat, visceral fat, and subcutaneous fat volumes were significantly different between the weight cycling group and the weight gain group (Figure 3C–E) ($p<0.05$). Therefore, weight cycling increases body weight, and the weight of liver and adipose tissue. To determine the systemic metabolic consequences of weight cycling, measurements of fasting blood glucose and total cholesterol were performed (Figure 4A, B). The fasting glucose and total cholesterol levels were significantly increased in the weight cycling group compared to the weight gain group ($p<0.05$). Taken together, the mice in the weight cycling group increased their body weights and the weight of their liver and adipose tissues, causing systemic metabolic dysfunction through high levels of blood glucose and total cholesterol.

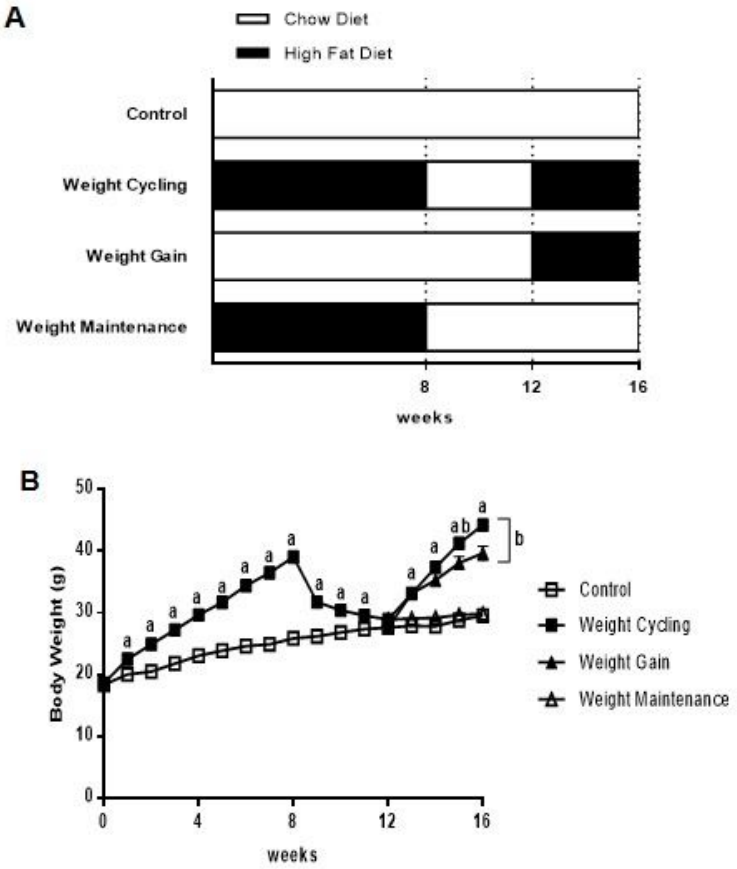

Figure 2. Study design and body weight changes.

(A) Study design for weight cycling. Male C57BL/6N mice were placed on a chow diet or a high fat diet for 8-4-4 week intervals. (Open bar: chow diet feeding, Shaded bar: high fat diet feeding) (B) Body weight for the duration of the study. Data are presented as the mean ± SEM; n = 15/group. (□: Control group, ■: Weight cycling group, ▲: Weight gain group, △: Weight maintenance group) Significance level set as $p<0.05$. **a** Significantly different from the control group at the same time

point. b Significantly different from the weight cycling group at the same time point.

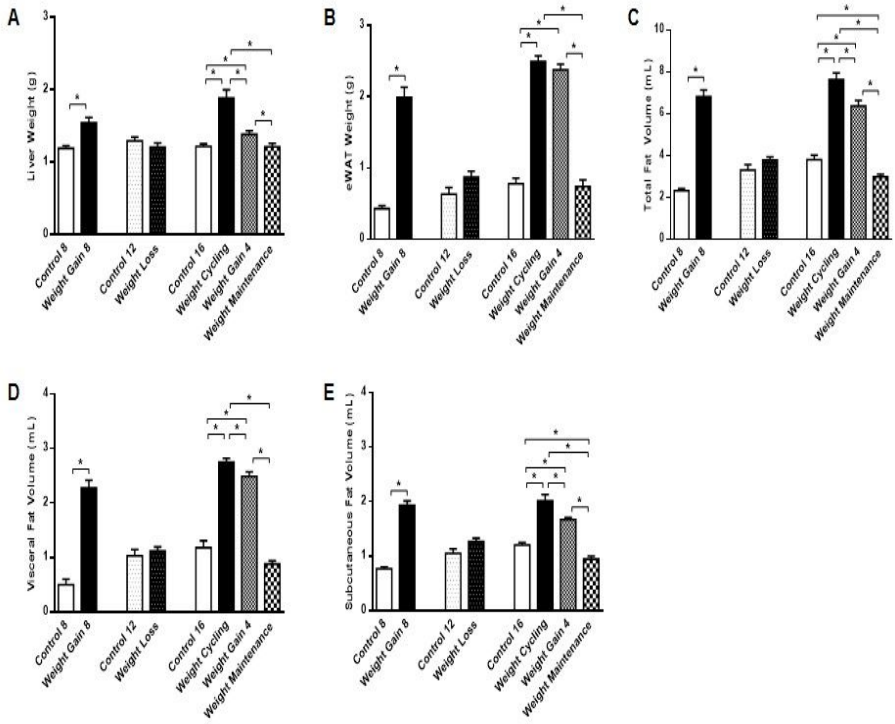

Figure 3. Weight cycling effects on organ weight.

Liver and adipose tissue weights were determined after 8, 12, and 16 weeks on a diet. (A) Liver weight and (B) epididymal adipose tissue weight (eWAT) were measured. (C) Total fat, (D) visceral fat and (E) subcutaneous fat volume were measured. Data are presented as the mean ± SEM; n = 10/group. Significance level set as $p<0.05$. * Significantly different from the following lines.

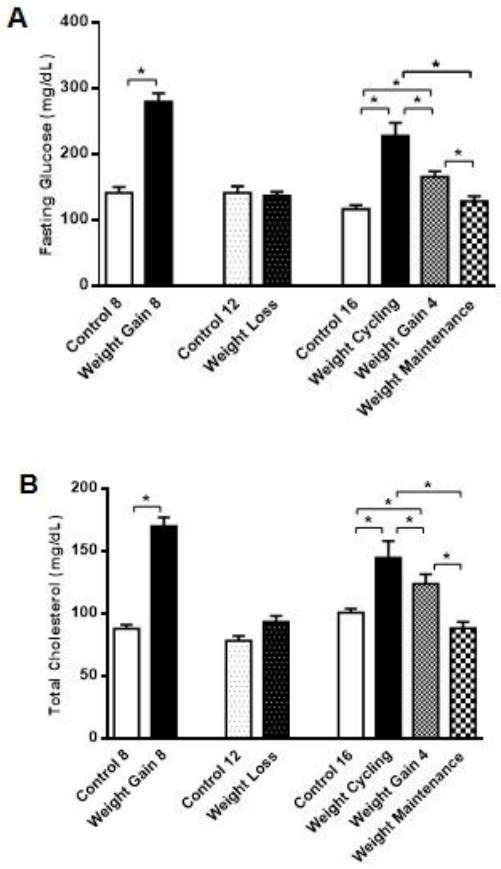

Figure 4. Weight cycling effects on blood metabolic parameters.

Metabolic parameters were evaluated at 8, 12, and 16 weeks of diet-challenged groups, following 12 h fasting. (A) Fasting glucose and (B) total cholesterol concentration. Data are presented as the mean ± SEM; n = 10/group. Significance level set as $p<0.05$. * Significantly different from the following lines.

2. Histology of liver and adipose tissue from weight cycling mice

To determine the influences of increased liver and adipose tissue weight on the group of weight cycling mice, we first investigated the histopathological changes in the liver. The livers of the mice in the weight cycling group were pale in color, and they were enlarged relative to those of the weight gain group (Figure 5A). Extensive hepatic steatosis developed in weight cycling group mice, with more advanced accumulation of lipid droplets, and with macro- and micro-vesicular steatosis (Figure 5B). Consistent with these findings, the weight cycling group had an increased hepatic triglyceride level (Figure 5C). These results suggest that weight cycling had impaired the metabolic functions of the liver, particularly in lipid metabolism. It is well known that a high fat diet increases both adipocyte size and adipose tissue mass, and that enlarged adipocytes are more insulin resistant. We performed histological observations of epididymal white adipose tissue (Figure 6A, top of panel). Adipocyte size was significantly increased in the weight cycling group compared to the weight gain group (Figure 6B) ($p<0.05$). Immune cells surround dying adipocytes and form characteristic 'crown-like structures' (Murano *et al*, 2008). The adipose tissue of the mice in the weight cycling group was characterized by immunohistochemistry staining. Dead adipocytes surrounded by M1 macrophages were identified as having F4/80-positive and CD11c-positive signals (Figure 6A, middle and lower of panel). Interestingly, the number of crown-like structures was increased in the weight cycling group compared to the weight gain group

(Figure 6C) ($p<0.05$). Therefore, weight cycling increased hypertrophic adipocytes and crown-like structures contributing to adipose tissue inflammation.

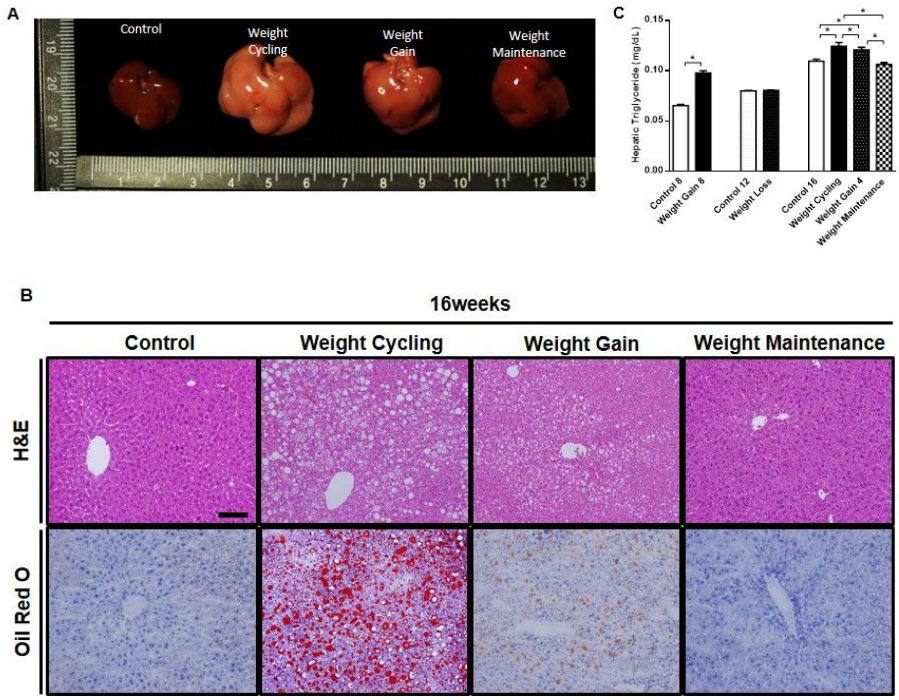

Figure 5. Histopathological analysis of liver sections from weight cycling mice.

Liver section analysis at 16 weeks of a diet-challenge. (A) Liver autopsy image at 16 weeks on a diet. (B) Representative images of liver sections stained with H&E and Oil Red O at 16 weeks of a diet-challenge (×200 magnification, scale bar size = 100 μm). (C) Hepatic triglyceride concentration was determined after 8, 12, and 16 weeks on a diet. Data are presented as the mean ± SEM; n = 10/group. Significance level set as $p<0.05$. * Significantly different from the following lines.

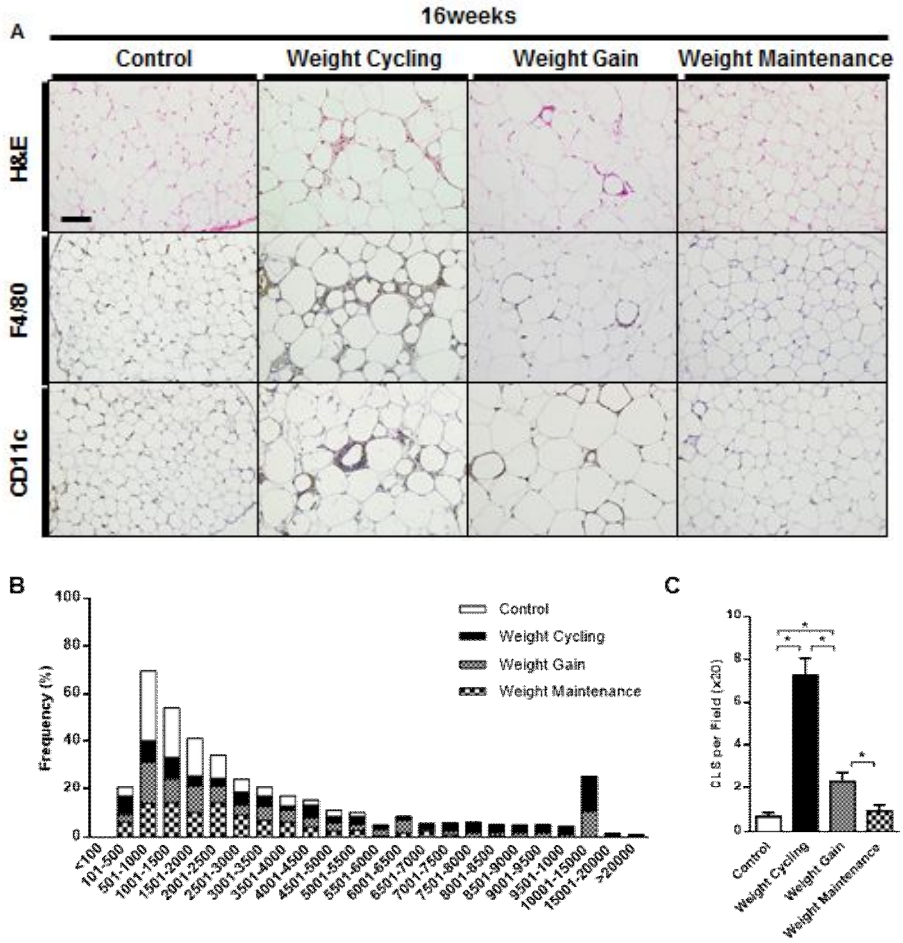

Figure 6. Histopathological analysis of epididymal white adipose tissue (eWAT) from weight cycling mice.

Epididymal white adipose tissue (eWAT) section analysis at 16 weeks of diet-challenge. (A) Representative images of eWAT sections stained with H&E, and immunohistochemistry with antibodies (dilution 1:100; F4/80, dilution 1:50, CD11c) (×200 magnification, scale bar size = 100 μm). (B) Adipocyte size

distribution and (C) crown-like structure (CLS) numbers counted. (Open bar: Control group, Shaded bar: Weight cycling group, Stippled bar: Weight gain group, Striped bar: Weight maintenance group) Data are presented as the mean ± SEM; n = 10/group. Significance level set as $p<0.05$. * Significantly different from the following lines.

3. Immune cell invasion in adipose tissue of weight cycling mice

Innate immune cells, including macrophages, are involved in adipose tissue inflammation. Macrophage accumulation in the adipose tissue of obese mice contributes to the development of insulin resistance (Shah, 2007). To determine whether weight cycling modulates innate immune cells in adipose tissue, the innate immune cell population present in adipose tissue was quantified using flow cytometry, and displayed in a scatter plot (Figure 7A). Both the total number of macrophages, and the number of M1 macrophages in particular, were significantly increased in the weight cycling group compared to the weight gain group (Figure 7B) ($p<0.05$). The number of M2 macrophages was increased in the weight cycling group as a results of the increasing total macrophage number (Figure 7B). Consistent with the findings for the macrophage subpopulation, the numbers of dendritic cells and natural killer cells were also increased in the weight cycling group compared to the weight gain group (Figure 7B, C). In addition, the M1 to M2 ratio was increased in the weight cycling group relative to the weight gain group (Figure 7D) ($p<0.05$). Therefore, weight cycling modulated the activation of M1 macrophages. These data indicate that weight cycling increases the populations of innate immune cells. In a previous study, the T cell subset was also found to accumulate in adipose tissue during obesity and to contribute to the development of insulin resistance (Yang *et al.*, 2010). Adaptive immune cell populations are shown in a scatter plot (Figure 8A). The weight cycling group had an increased number

of B cells and an increased total number of T cells, including $CD4^+$ T cells, compared to the weight gain group (Figure 8B) ($p<0.05$). In contrast, the number of regulatory T cells (Treg), which are involved in anti-inflammatory responses, was not different between the weight cycling group and the weight gain group (Figure 8B). The Treg to $CD4^+$ T cell ratio was significantly decreased in the weight cycling group relative to the weight gain group (Figure 8C) ($p<0.05$). The inflammation of adipose tissue achieved by weight cycling is affected by $CD4^+$ T cells. These data indicate that the population levels of both innate and adaptive immune cells influence adipose tissue inflammation in weight cycling mice.

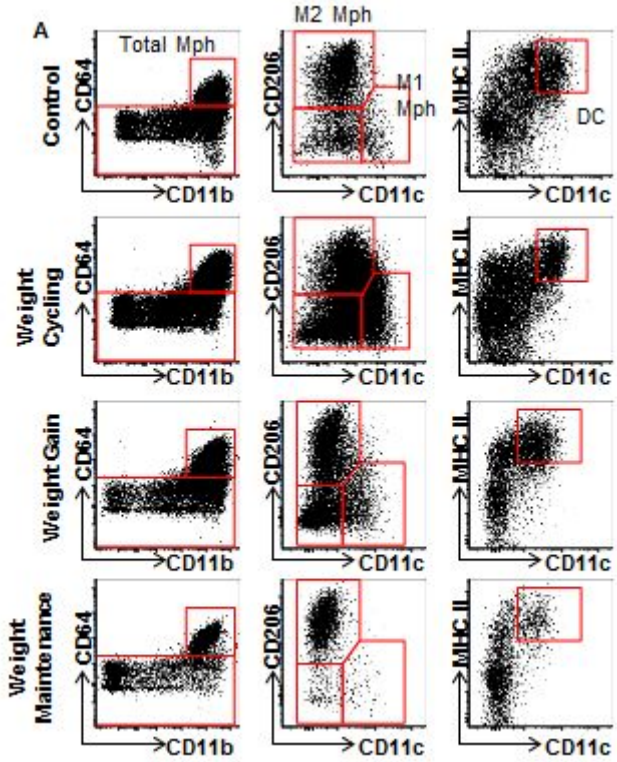
A
Total Mph
M2 Mph
M1 Mph
DC
Control
Weight Cycling
Weight Gain
Weight Maintenance
CD64
CD11b
CD206
CD11c
MHC II
CD11c

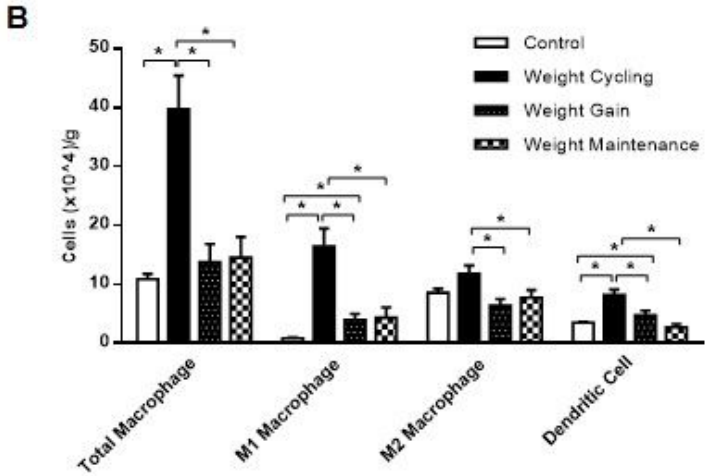
B
Control
Weight Cycling
Weight Gain
Weight Maintenance
Cells (x10^4)/g
50
40
30
20
10
0
Total Macrophage
M1 Macrophage
M2 Macrophage
Dendritic Cell

Continued Figure 7.

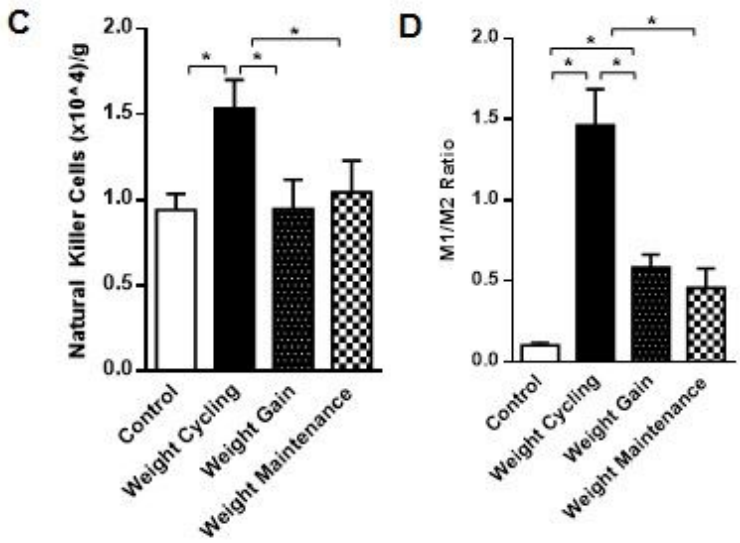

Figure 7. FACS analysis of innate immune cell population in the adipose tissue of weight cycling mice.

Stromal vascular fraction cells were isolated from epididymal adipose tissue, and analyzed by flow cytometry. Innate immune cell population analysis at 16 weeks of diet-challenge. Cells were gated for the innate immune cell population based upon forward and side scatter, and analyzed for each immune cell marker. (A) Macrophage subpopulation scatter plots, gated by CD64 and CD11b, represent total macrophages. CD11c-positive cells (M1 macrophages) and CD206-positive cells (M2 macrophages) were analyzed. MHC Ⅱ and CD11c-positive cells were dendritic cells. The gating strategy for natural killer cells is provided in Figure 1. (B) Innate immune cell population, and (C) natural killer cells

were counted in cells per gram. (Open bar: Control group, Shaded bar: Weight cycling group, Stippled bar: Weight gain group, Striped bar: Weight maintenance group) (D) M1 to M2 ratio at 16 weeks of diet-challenge. Data are presented as the mean ± SEM; n = 10-12/group. Significance level set as $p<0.05$. * Significantly different from the following lines.

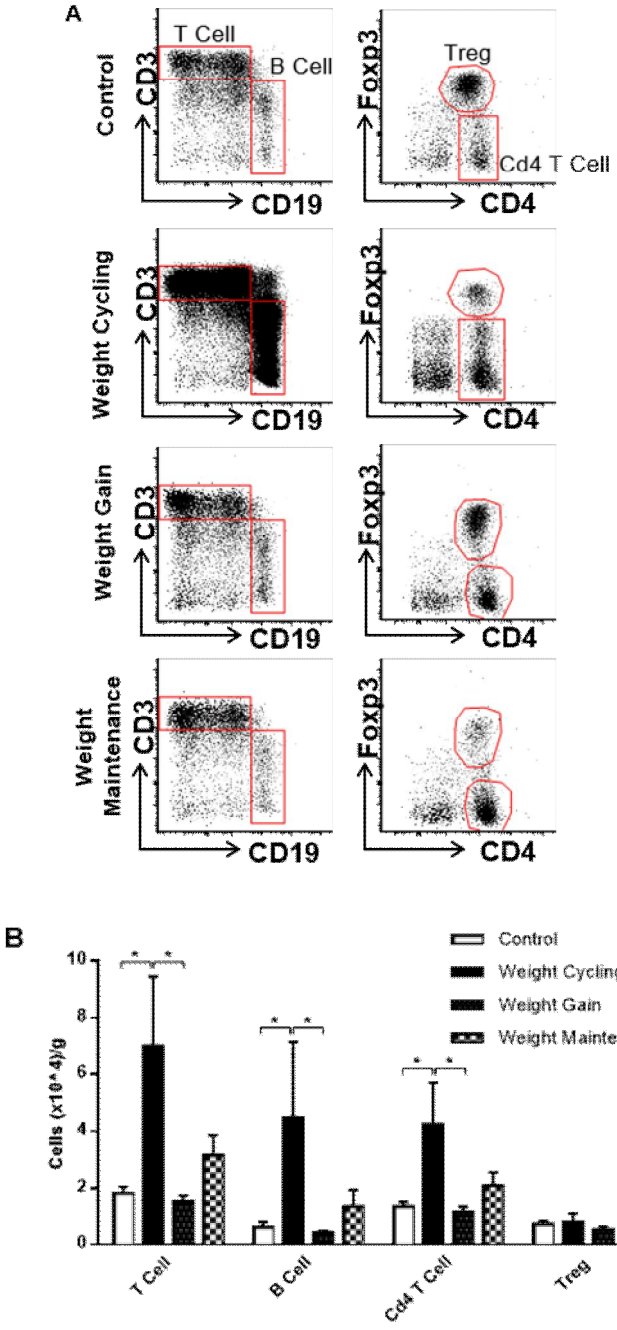
A
T Cell
B Cell
Control
CD3
CD19
Treg
Foxp3
Cd4 T Cell
CD4
Weight Cycling
Weight Gain
Weight Maintenance
B
Control
Weight Cycling
Weight Gain
Weight Maintenance
Cells (x10^4)/g
10
8
6
4
2
0
T Cell
B Cell
Cd4 T Cell
Treg

Continued Figure 8.

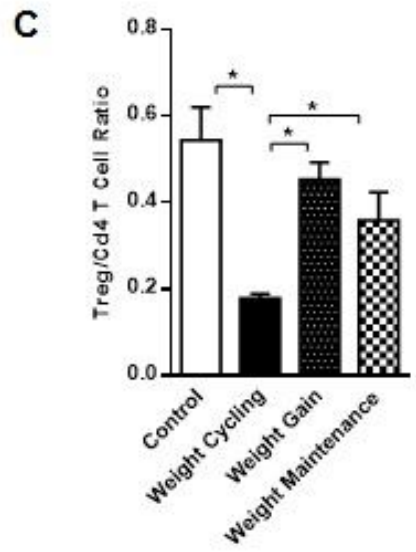

Figure 8. FACS analysis of adaptive immune cell population in the adipose tissue of weight cycling mice.

Stromal vascular fraction cells were isolated from epididymal adipose tissue and analyzed by flow cytometry. Analysis of the adaptive immune cell population at 16 weeks of diet-challenge. (A) Scatter plots of the adaptive immune cell population, gated using CD3 and CD19, to identify T cells and B cells. CD3-positive gated cells were analyzed for Foxp3, CD4-Foxp3-positive cells (Regulatory T cells, Treg), and CD4-positive cells ($CD4^+$ T cells) were analyzed. (B) The adaptive immune cell population was counted in cells per gram. (Open bar: Control group, Shaded bar: Weight cycling group, Stippled bar: Weight gain group, Striped bar: Weight maintenance group) (C) Treg to $CD4^+$ T cell ratio at 16 weeks of

diet-challenge. Data are presented as the mean ± SEM; n = 10-12/group. Significance level set as $p<0.05$. * Significantly different from the following lines.

4. Differential gene expression in the adipose tissue of weight cycling mice

In addition to the FACS data, real-time PCR analysis demonstrates that weight cycling influences immune cell gene expression, and the expression of inflammatory cytokines in particular. Consistent with the FACS data, a general macrophage marker (*F4/80*), and markers specific for M1 macrophages (*MCP1, NOS2, Mgl1*), gave increased expressions in the weight cycling group compared to the weight gain group (Figure 9A - D). In contrast, the signals from markers specific for M2 macrophages (*Ym1, ARG1*), were not different between the weight cycling group and the weight gain group (Figure 9E, F). The expression of a dendritic cell marker (*Itgax*) was increased in the weight cycling group compared to the control group, while that expression level was the same in the weight gain group (Figure 9G). The expression of markers for $CD4^+$ T cells (*CD4*), and B cells (*CD19*) was significantly increased in the weight cycling group compared to the weight gain group (Figure 9H, I) ($p<0.05$). The expression of *Foxp3*, a Treg marker, did not differ between the weight cycling group and the weight gain group (Figure 9J). To investigate the inflammatory state of immune cells in the adipose tissue, the expression of inflammatory cytokines was assessed. The expression of pro-inflammatory cytokines (*IFNγ, TNF-α, IL-6*) was significantly increased in the weight cycling group compared to the weight gain group (Figure 9K - M) ($p<0.05$). The expression of anti-inflammatory cytokines (*IL-10, IL-4*) was increased (Figure 9N, O), while the expression of adiponectin was significantly decreased, in the

weight cycling group compared to the weight gain group (Figure 9P) ($p<0.05$). Taken together, these results demonstrate that the immune response of the weight cycling group is affected by both innate and adaptive immune cells, and by inflammatory cytokines released by these cells. To determine which genes had an elevated expression in the adipose tissue of the weight cycling group, we sorted genes from mRNA sequencing data (GEO profiles database, GSE73345) by their expression level in the adipose tissue of the weight cycling group. We selected genes associated with immune responses, enriched in adipose tissue, and whose expression was increased in the weight cycling group compared to the weight gain group (Table 5). Gene expression was increased in both the weight cycling group and the weight gain group (Figure 10A). Genes expressed in both adipose tissue and stromal vascular fraction were contained in the immune cell population. The adipose tissue, from mice in the 4-week high fat diet group, was collected and adipocytes and the stromal vascular fraction were separated. Gene expression was quantified using RT-PCR (Figure 10B-H). The expression levels of *Irgm2*, *Nkg7* and *C1qc* were increased in adipocytes from mice in the high fat diet group, compared to mice in the chow diet group (Figure 10B, D, and G). In contrast, the expression of *Gbp2* and *H2-DMb1* was increased in the stromal vascular fraction of mice in the high fat diet group (Figure 10C, H). There was no difference in the expression level of *H2-Aa* or *CD3g,* in adipocytes or in the stromal vascular fraction (Figure 10E, F). Taken together, these findings demonstrate that *Irgm2*, *Nkg7* and *C1qc* were mainly regulated by adipocytes, while *Gbp2* and *H2-DMb1* were regulated by stromal vascular fraction immune

cells. These finding suggest that an altered immune-related gene expression in adipose tissue may contribute to adipose tissue inflammation during weight cycling.

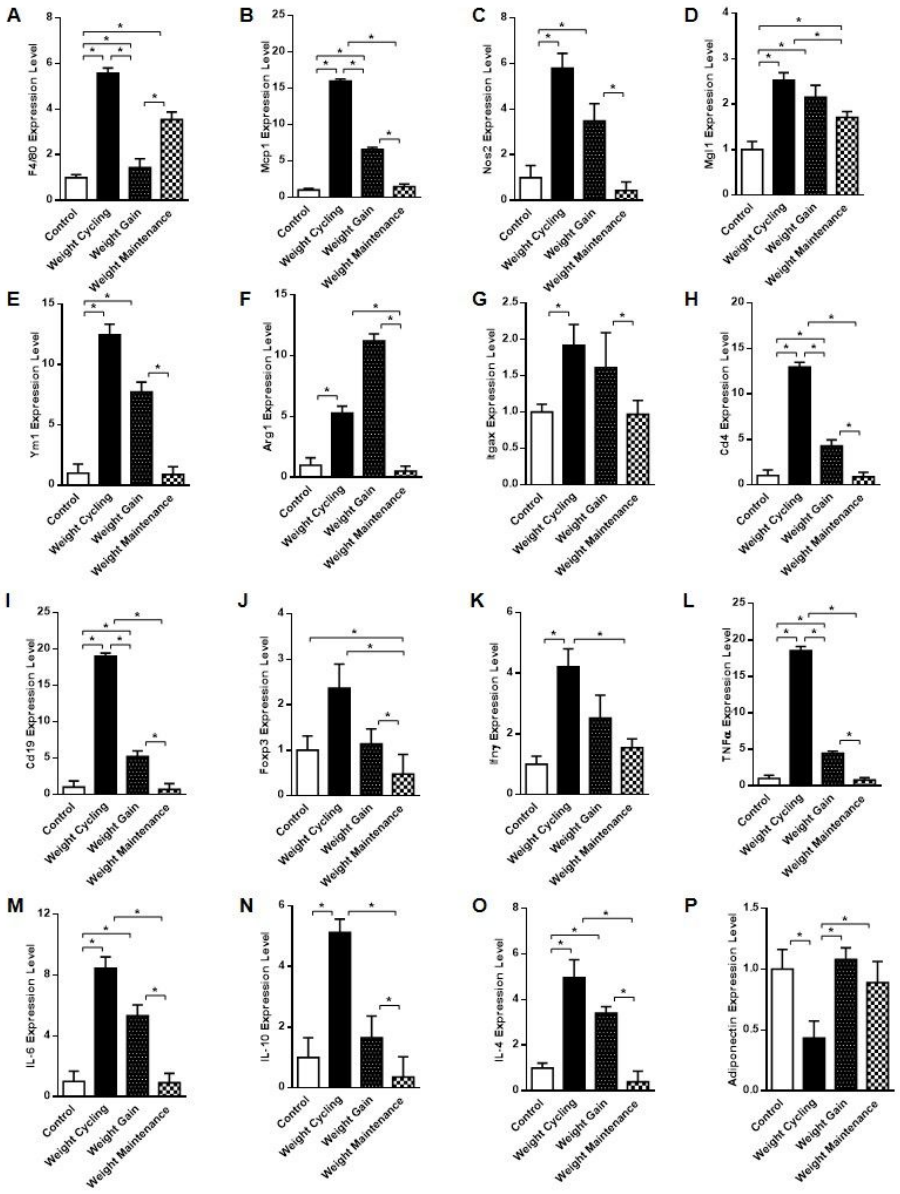

Figure 9. Gene expression of immune cell markers and cytokines in the adipose tissue of weight cycling mice.

RNA was isolated from epididymal white adipose tissue. Gene expression was analyzed by real-time RT-PCR. A - J: Expression of immune cell markers in adipose tissue. K - P: Expression levels of inflammatory cytokines in adipose tissue. (A) *F4/80* (B) *MCP1* (C) *NOS2* (D) *Mgl1* (E) *Ym1* (F) *ARG1* (G) *Itgax* (H) *CD4* (I) *CD19* (J) *Foxp3* (K) *IFNγ* (L) *TNF-α* (M) *IL-6* (N) *IL-10* (O) *IL-4* (P) *Adiponectin*. Data are presented as the mean ± SEM; n = 10-12/group. Significance level set as $p<0.05$. * Significantly different from the following lines.

Table 5. List of genes with altered expression in the adipose tissue of weight cyling mice

Gene symbol	Description	Function	logFC[1)]
Irgm2	Immunity-related GTPase family M protein 2	Autophagy	2.22
Nkg7	Natural killer cell group 7 sequence	Unknown function	2.14
CD3g	T-cell surface glycoprotein CD3 gamma	T cell receptor	2.02
Gbp2	Interferon-induced guanylate-binding protein 2	Antiviral activity	1.62
C1qc	Complement C1q subcomponent subunit C	Innate immune response	1.19
H2-DMb1	Class Ⅱ histocompatibility antigen, M beta 1 chain	MHC class Ⅱ	0.88
H2-Aa	H-2 class Ⅱ histocompatibility antigen, A-K alpha chain	MHC class Ⅱ	0.71

Altered gene selection data from GEO profiles database (GSE73345).

[1)] Log fold value change in weight cycling group compared with weight gain group

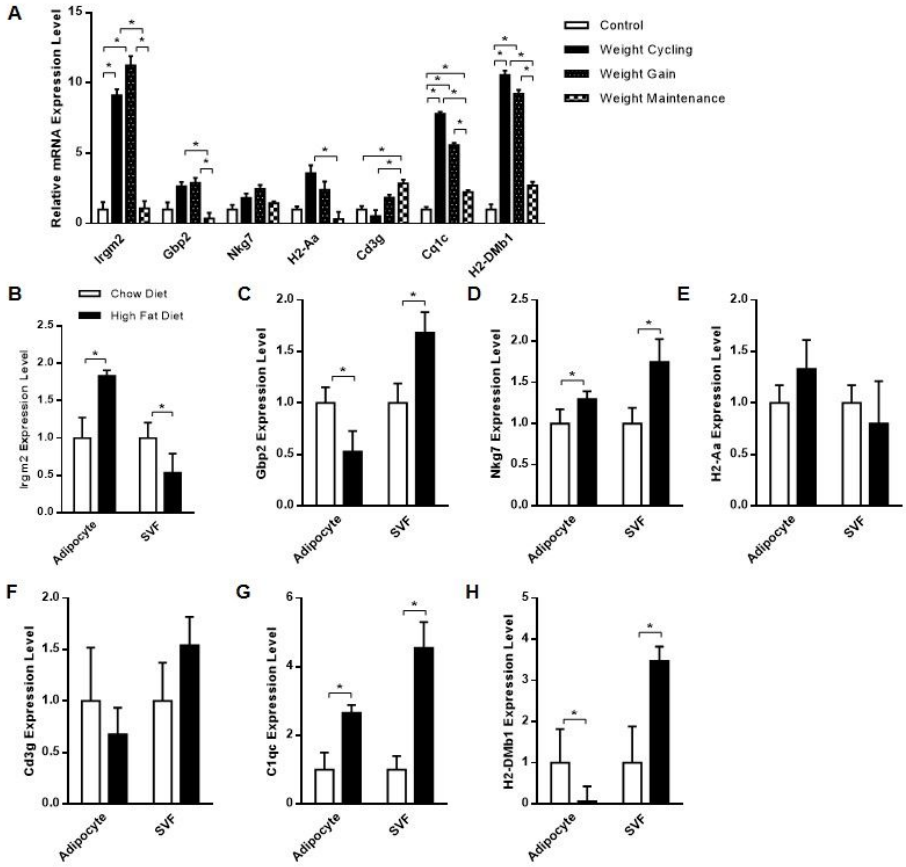

Figure 10. Altered gene expression in adipose tissue of weight cycling mice.

Altered genes were selected from Table 5. RNA was isolated from epididymal white adipose tissue. Gene expression was analyzed by real-time RT-PCR. (A) Altered gene expression levels at 16 weeks of diet-challenge. (Open bar: Control group, Shaded bar: Weight cycling group, Stippled bar: Weight gain group, Striped bar: Weight maintenance group) B - H: After mice

had been fed either a chow diet or a high fat diet for 4 weeks, their epididymal white adipose tissue was isolated. Adipocytes and the stromal vascular fraction were immediately separated, and RNA was isolated. (B) *Irgm2*. (C) *Gbp2*. (D) *Nkg7*. (E) *H2-Aa*. (F) *CD3g*. (G) *C1qc*. (H) *H2-DMb1*. Data are presented as the mean ± SEM; n = 10-12/group. Significance level set as $p<0.05$. * Significantly different from the following lines.

Ⅳ. Discussion

Obesity is associated with low-grade chronic inflammation attributed to dysregulated production/release of cytokines and adipokines, to dyslipidemia, and to disrupted glucose-insulin homeostasis (J, Lee., 2013). Nutritional interventions, such as dieting, are often accompanied by repeated bouts of weight loss and regain, a phenomenon known as weight cycling (Brownell KD, Greenwood MR, Stellar E & EE., 1986). The purpose of this study, is to clarify the differences between inducing obesity with weight cycling, and gaining weight without cycling. In this paper, the mice in the weight cycling group exhibited an aggravated metabolic phenotype compared to mice in the weight gain group. Mice in the weight cycling group had an increased body weight and liver weight, and adipose tissue volume. In a previous study, the adipose tissue depot of a group of mice undergoing weight cycling was significantly increased compared to control groups (Dankel SN *et al.*, 2014). Additionally, body weight and energy balance are key contributors to systemic glucose levels (Coenen, Gruen, Chait, & Hasty, 2007). We established the levels of several biochemical in the serum of weight cycling mice. Interestingly, the fasting blood glucose level and the total cholesterol level were significantly increased in the weight cycling group, compared to the weight gain group. In a previous study, it was established that weight cycling impairs systemic glucose tolerance (Anderson EK, Gutierrez DA, Kennedy A & AH., 2013). Additional studies will be needed to establish whether the increases in the blood glucose level and total cholesterol

affect the insulin signaling pathway that maintains glucose homeostasis. In a previous study, it was found that liver damage could not be reversed in mice during the lean period of diet-induced weight cycling (Barbosa-da-Silva, da Silva, Aguila, & Mandarim-de-Lacerda, 2014). On the other hand, our data demonstrate that weight loss ameliorates hepatic steatosis and the accumulation of hepatic triglycerides. The livers from weight cycling mice have a bright color, an increased weight, and display lipid accumulation. Therefore, weight cycling influences hepatic lipid metabolism. Consistent with the findings in the liver, the weight of adipose tissue in mice from the weight cycling group was increased compared to that in weight gain group. Obesity leads to chronic inflammation, driven by the immune system that promotes insulin resistance and type 2 diabetes in rodents and humans. This inflammation is characterized by an influx of inflammatory immune cells into metabolic tissues, such as adipose tissue (Weisberg *et al.*, 2003; Xu *et al.*, 2003; Shu, Benosit, & Mathis, 2012). Compared to mice in the weight gain group, the mice in the weight cycling group had an increased adipose tissue weight and an increased number of hypertrophic adipocytes. Interestingly, the number of crown-like structures increased in the adipose tissue of the mice in the weight cycling group. The tissue localization of macrophages in adipose tissue is known to be an indicator of their function, with cells located in crown-like structures showing greater inflammatory potential. Additionally, macrophages in crown-like structures possess a pro-inflammatory phenotype (Lumeng, Bodzin, & Saltiel, 2007; Cinti S *et al.*, 2005). M1 macrophage mediated pro-inflammatory immune responses were increased in the adipose tissues of mice

in the weight cycling group. Consistent with the histopathological data, FACS analysis demonstrated that the adipose tissues of weight cycling mice contain an increased population of invasive immune cells. In a previous study, it was found that weight cycling enhances the inflammatory responses of adipose tissue in male mice, through alterations in inflammatory adipokines (Barbosa-da-Silva, da Silva, Aguila, & Mandarim-de-Lacerda, 2014). Additionally, a T cell-driven inflammatory response may contribute to the metabolic abnormalities associated with weight cycling, and neither adipose tissue macrophage number nor polarization were modulated by weight cycling (Anderson EK, Gutierrez DA, Kennedy A, & AH., 2013). Interestingly, we demonstrated that total macrophage numbers, and the number of M1 macrophages in particular, are increased in adipose tissue from the weight cycling group, compared to that from the weight gain group. The M1 to M2 macrophage ratio is increased in adipose tissue from the weight cycling group. Therefore, M1 macrophage activation is more prominent that that of M2 macrophages. Our data concerning the immune cell populations in the weight cycling group differs slightly from that in previous reports. These differences may arise from different animal procedures, including the duration and composition of the diets.

M1 macrophages are the most important immune cells for the induction of inflammation in adipose tissue (Fujisaka *et al.*, 2009). Recent evidence indicates that, in addition to macrophages, other innate immune cells become increased during obesity-associated insulin resistance, including dendritic cells and natural killer cells (Bertola *et al.*, 2012; Wensveen *et al.*, 2015). Here we demonstrate that the adipose tissue of mice in the weight cycling

group contains an increased number of dendritic cells and natural killer cells. Therefore, inflammation of adipose tissues in weight cycling mice is influenced by elevated innate immune cell populations. T cells also accumulate in adipose tissue during obesity and contribute to the development of insulin resistance (Wu *et al.*, 2007). In particular, B cells were shown to promote inflammation and regulate T cell function during obesity in a previous study (DeFuria J *et al.*, 2013). Similarly, we confirmed that adaptive immune cells, including total T cells, $CD4^+$ T cells, and B cells, become increased in the adipose tissue of mice from the weight cycling group compared that tissue from mice in the weight gain group. No difference was seen in the role of anti-inflammatory of Treg cells between the weight cycling group and the weight gain group. The Treg to $CD4^+$ T cell ratio in adipose tissue is increased in the group of weight cycling mice relative to the weight gain group. Therefore, inflammation of adipose tissue in the weight cycling group is influenced by $CD4^+$ T cell activation. In a previous study, it was found that macrophages in adipose tissue function as antigen-presenting cells, and that they regulate $CD4^+$ T cells with in adipose tissue in mice (MorrisDL *et al.*, 2013). Additionally, an MHC-2 dependent activation loop, between macrophages in adipose tissue and $CD4^+$ T cells, controls obesity-induced inflammation (Cho *et al.*, 2014). The increased inflammation of adipose tissue in the weight cycling group is caused by the interaction of macrophages and $CD4^+$ T cells. Moreover, obesity contributes to increased circulating levels of pro-inflammatory cytokines, suchas TNF-α, IFNγ, and IL-6 (Makki K, Froguel P & I, 2013). A pro-inflammatory state arises from an unbalanced pro- and/or

anti-inflammatory cytokine level (Jung & Choi, 2014). In the current study, pro-inflammatory cytokine expression is increased in the adipose tissue of the weight cycling group, compared to the weight gain group. The anti-inflammatory cytokine level was not significantly different between the weight cycling group and the weight gain group. Consistent with the increased number of invasive immune cells in the adipose tissue of the weight cycling group, immune cell activation is increased in the adipose tissue of the weight cycling group compared to the weight gain group. Taken together, these results demonstrate that the adipose tissue of the weight cycling group contains an increased population of invasive immune cells, including both innate and adaptive immune cells, and that the adipose tissue entered a pro-inflammatory state.

To our knowledge, there are few previous studies that have investigated the correlation between adipose tissue inflammation and altered gene expression during weight cycling. In the current study, we compared gene expression patterns in adipose tissue between the weight cycling group and the weight gain group. Genes with elevated expressions were mainly those involved in immune responses, and they were enriched in adipose tissue. To elucidate the role of the elevated genes in the different adipogenic behavior seen between the weight cycling group and the weight gain group, the gene expression level was re-confirmed separately in adipose tissue and in the stromal vascular fraction by RT-PCR. The expression of *Irgm2* is increased in adipocytes and decreased in the stromal vascular fraction of mice fed a high fat diet. In contrast, the expression of *Gbp2* and *H2-DMb1* is decreased in adipocytes and increased in the stromal vascular

fraction of mice fed a high fat diet. Furthermore, the expression of *Nkg7* and *C1qc* is increased in both adipocytes and the stromal vascular fraction of mice fed a high fat diet. Altered gene expression affects different cell types present in adipose tissue. It was well known that *Irgm2* is involved in the innate immune response, regulating autophagy formation in response to intracellular pathogens, such as *Toxoplasma gondii* (Hunn JP *et al.*, 2008). Autophagy is involved in inflammation, endoplasmic reticulum stress and the monocyte chemoattractant protein-1/CCR2 pathway (Nunez *et al.*, 2013). Our results demonstrate that the adipose tissue of weight cycling mice promotes increased macrophage activation. *Irgm2* is associated with adipose tissue inflammation in weight cycling. Additionally, *Gbp2* is influenced by the localization by Irgm protein, modulating macroautophagy (Kolattukudy & Niu, 2012). Obesity is also associated with defective regulation of autophagy in adipose tissue (Traver *et al.*, 2011). The expression of *Irgm2* and *Gbp2* is increased in the adipose tissue of weight cycling mice. Therefore, adipose tissue inflammation in the weight cycling group is increased, correlating with the regulation of autophagy. Additional studies are needed to confirm this hypothesized association between the autophagy signaling pathway and the gene expression pattern in weight cycling mice. *Nkg7* is a type I membrane protein, however its function remains unknown. According to a previous study, *Nkg7* may be involved in a specific function elicited by IL-2 stimulation of natural killer cells (Mori S *et al.*, 1998). The function of IL-2 is related to the division of T cells and B cells, and the activation of monocytes and natural killer cells. Natural killer cells link obesity-induced

adipose stress to inflammation and insulin resistance (Wensveen *et al.*, 2015). Natural killer cells are increased in the adipose tissues of the weight cycling group, compared to the weight gain group. Additional experiments are needed to determine the impact *Nkg7* on immune cells, and on adipose tissue inflammation, in the weight cycling group.

Our study investigated the differences between the weight cycling group and weight gain group. Mice in the weight cycling group have an aggravated metabolic phenotype, and an increased number of invasive immune cells, including both innate and adaptive immune cells. Our results suggest the possibility that differences in the degree of metabolic aggravation between the weight cycling group and the weight gain group, are contributed to by cells from both the adaptive and innate immune system. Pro-inflammatory state occurs in the adipose tissue of weight cycling mice. In addition, the expression of multiple immune-related genes, and pro-inflammatory cytokine genes in particular, become elevated subsequent to weight cycling, compared to the weight gain group. Altered immune cell populations, and their gene expression patterns in adipose tissue, may contribute to metabolic aggravation during weight cycling. Further studies will be needed to investigate in greater detail the mechanisms of adaptive and innate immunity that lead to the differing adipose inflammation in weight cycling mice.

Reference

Anderson, E.K., Gutierrez, D.A., Kennedy, A., and Hasty, A.H. (2013). Weight cycling increases T-cell accumulation in adipose tissue and impairs systemic glucose tolerance. Diabetes 62, 3180-3188.

Barbosa-da-Silva, S., Fraulob-Aquino, J.C., Lopes, J.R., Mandarim-de-Lacerda, C.A., and Aquila, M.B. (2012). Weight cycling enhances adipose tissue inflammatory responses in male mice. PLos One. 7, e39837.

Barbosa-da-Silva, S., da Silva, N.C., Aguila, M.B., and Mandarim-de-Lacerda, C.A. (2014). Liver damage is not reversed during the lean period in diet-induced weight cycling in mice. Hepatol Res 44, 450-459.

Bertola, A., Ciucci, T., Rousseau, D., Bourlier, V., Duffaut, C., Bonnafous, S., Blin-Wakkach, C., Anty, R., Iannelli, A., Gugenheim, J., Tran, A., Bouloumie, A., Gual, P., and Wakkach, A. (2012). Identification of adipose tissue dendritic cells correlated with obesity-associated insulin-resistance and inducing Th17 responses in mice and patients. Diabetes 61, 2238-2247.

Blackburn, G.L., Wilson, G.T., Kanders, B.S., Stein, L.J., Lavin, P.T., Adler, J., and Brownell, K.D. (1989). Weight cycling: the experience of human dieters. Am J Clin Nutr 49, 1105-1109.

Brownell, K.D., Greenwood, M.R., Stellar, E., and Srager, E.E. (1986). The effects of repeated cycles of weight loss and regain in rats. Physiol Behav 38, 459-464.

Cho, K.W., Morris, D.L., DelProposto, J.L., Geletka, L., Zamarron, B., Martinez-Santibanez, G., Meyer, K.A., Singer, K., O'Rourke, R.W., and Lumeng, C.N. (2014). An MHC II-dependent activation loop between adipose tissue macrophages and CD4+ T cells controls obesity-induced inflammation. Cell Reports 9, 605-617.

Cinti, S., Mitchell, G., Barbatelli, G., Murano, I., Ceresi, E., Faloia, E., Wang, S., Fortier, M., Greenberg, A.S., and Obin, M.S. (2005). Adipocyte death defines macrophage localization and function in adipose tissue of obese mice and humans. J Lipid Res 46, 2347-2355.

Cipolletta, D., Kolodin, D., Benoist, C., and Mathis, D. (2011). Tissular T(regs): a unique population of adipose-tissue-resident Foxp3+CD4+ T cells that impacts organismal metabolism. Semin Immunol 23, 431-437.

Coenen, K.R., Gruen, M.L., Chait, A., and Hasty, A.H. (2007). Diet-induced increases in adiposity, but not plasma lipids, promote macrophage infiltration into white adipose tissue. Diabetes 56, 564-573.

Dankel, S.N., Degerud, E.M., Borkowski, K., Fjære, E., Midtbø, L.K., Haugen, C., Solsvik, M.H., Lavigne, A.M., Liaset, B.,

Sagen, J.V., Kristiansen, K., Mellgren, G., and Madsen, L. (2014). Weight cycling promotes fat gain and altered clock gene expression in adipose tissue in C57BL/6J mice. Am J Physiol Endocrinol Metab 306, E210-224.

de Luca, C., and Olefsky, J.M. (2008). Inflammation and insulin resistance. FEBS Lett. 582, 97-105.

DeFuria, J., Belkina, A.C., Jagannathan-Bogdan, M., Snyder-Cappione, J., Carr, J., Nersesova, Y.R., Markham, D., Strissel, K.J., Watkins, A.A., Zhu, M., Allen, J., Bouchard, J., Toraldo, G., Jasuja, R., Obin, M.S., McDonnell, M.E., Apovian, C., Denis, G.V., and Nikolajczyk, B.S. (2013). B cells promote inflammation in obesity and type 2 diabetes through regulation of T-cell function and an inflammatory cytokine profile. PNAS 110, 5133-5138.

Fujisaka, S., Usui, I., Bukhari, A., Ikutani, M., Oya, T., Kanatani, Y., Tsuneyama, K., Nagai, Y., Takatsu, K., Urakaze, M., Kobayashi, M., and Tobe, K. (2009). Regulatory mechanisms for adipose tissue M1 and M2 macrophages in diet-induced obese mice. Diabetes 58, 2574-2582.

Hunn, J.P., Koenen-Waisman, S., Papic, N., Schroeder, N., Pawlowski, N., Lange, R., Kaiser, F., Zerrahn, J., Martens, S., and Howard, J.C. (2008). Regulatory interactions between IRG resistance GTPases in the cellular response to Toxoplasma gondii. EMBO J. 27, 2495-2509.

Lee, J. (2013). Adipose tissue macrophages in the development of obesity-induced inflammation, insulin resistance and type 2 diabetes. Arch Pharm Res 36, 208-222.

Jung, U.J., and Choi, M.S. (2014). Obesity and its metabolic complications: the role of adipokines and the relationship between obesity, inflammation, insulin resistance, dyslipidemia and nonalcoholic fatty liver disease. Int J Mol Sci 15, 6184-6223.

Kolattukudy, P.E., and Niu, J. (2012). Inflammation, endoplasmic reticulum stress, autophagy, and the monocyte chemoattractant protein-1/CCR2 pathway. Circ Res 110, 174-189.

Kosteli, A., Sugaru, E., Haemmerle, G., Martin, J.F., Lei, J., Zechner, R., and Ferrante, A.W., Jr. (2010). Weight loss and lipolysis promote a dynamic immune response in murine adipose tissue. J Clin Invest 120, 3466-3479.

Kraschnewski, J.L., Boan, J., Esposito, J., Sherwood, N.E., Lehman, E.B., Kephart, D.K., and Sciamanna, C.N. (2010). Long-term weight loss maintenance in the United States. Int J Obes 34, 1644-1654.

Li, P., Lu, M., Nguyen, M.T., Bae, E.J., Chapman, J., Feng, D., Hawkins, M., Pessin, J.E., Sears, D.D., Nguyen, A.K., Amidi, A., Watkins, S.M., Nguyen, U., and Olefsky, J.M. (2010). Functional heterogeneity of CD11c-positive adipose tissue macrophages in diet-induced obese mice. J Biol Chem 285,

15333-15345.

Lumeng, C.N. (2013). Innate immune activation in obesity. Mol Aspects Med 34, 12-29.

Lumeng, C.N., Bodzin, J.L., and Saltiel, A.R. (2007). Obesity induces a phenotypic switch in adipose tissue macrophage polarization. J Clin Invest 117, 175-184.

Makki, K., Froguel, P., and Wolowczuk, I. (2013). Adipose tissue in obesity-related inflammation and insulin resistance: cells, cytokines, and chemokines. ISRN inflamm 2013, 139239.

Mehta, T., Smith, D.L., Jr., Muhammad, J., and Casazza, K. (2014). Impact of weight cycling on risk of morbidity and mortality. Obese Rev 15, 870-881.

Mori, S., Jewett, A., Cavalcanti, M., Murakami-Mori, K., Nakamura, S., and Bonavida, B. (1998). Differential regulation of human NK cell-associated gene expression following activation by IL-2, IFN-alpha and PMA/ionomycin. Int J Oncol 12, 1165-1170.

Morris, D.L., Cho, K.W., Delproposto, J.L., Oatmen, K.E., Geletka, L.M., Martinez-Santibanez, G., Singer, K., and Lumeng, C.N. (2013). Adipose tissue macrophages function as antigen-presenting cells and regulate adipose tissue CD4+ T cells in mice. Diabetes 62, 2762-2772.

Murano, I., Barbatelli, G., Parisani, V., Latini, C., Muzzonigro, G., Castellucci, M., and Cinti, S. (2008). Dead adipocytes, detected as crown-like structures, are prevalent in visceral fat depots of genetically obese mice. J Lipid Res 49, 1562-1568.

Nishimura, S., Manabe, I., Nagasaki, M., Eto, K., Yamashita, H., Ohsugi, M., Otsu, M., Hara, K., Ueki, K., Sugiura, S., Yoshimura, K., Kadowaki, T., and Nagai, R. (2009). CD8+ effector T cells contribute to macrophage recruitment and adipose tissue inflammation in obesity. Nat Med 15, 914-920.

Nunez, C.E., Rodrigues, V.S., Gomes, F.S., Moura, R.F., Victorio, S.C., Bombassaro, B., Chaim, E.A., Pareja, J.C., Geloneze, B., Velloso, L.A., and Araujo, E.P. (2013). Defective regulation of adipose tissue autophagy in obesity. Int J Obes 37, 1473-1480.

Olefsky, J.M., and Glass, C.K. (2010). Macrophages, inflammation, and insulin resistance. Ann Rev Physiol 72, 219-246.

Kopelman, P. (2007). Health risks associated with overweight and obesity. Obes Rev 8, 13-17.

Rector, R.S., Warner, S.O., Liu, Y., Hinton, P.S., Sun, G.Y., Cox, R.H., Stump, C.S., Laughlin, M.H., Dellsperger, K.C., and Thomas, T.R. (2007). Exercise and diet induced weight loss improves measures of oxidative stress and insulin sensitivity in adults with characteristics of the metabolic syndrome. Am J Physiol Endocrinol Metab 293, E500-506.

Schipper, H.S., Prakken, B., Kalkhoven, E., and Boes, M. (2012). Adipose tissue-resident immune cells: key players in immunometabolism. Trends Endocrinol Metab 23, 407-415.

Shah, P.K. (2007). Innate immune pathway links obesity to insulin resistance. Circ Res 100, 1531-1533.

Shu, C.J., Benoist, C., and Mathis, D. (2012). The immune system's involvement in obesity-driven type 2 diabetes. Semin Immunol 24, 436-442.

Strissel, K.J., DeFuria, J., Shaul, M.E., Bennett, G., Greenberg, A.S., and Obin, M.S. (2010). T-cell recruitment and Th1 polarization in adipose tissue during diet-induced obesity in C57BL/6 mice. Obesity 18, 1918-1925.

Traver, M.K., Henry, S.C., Cantillana, V., Oliver, T., Hunn, J.P., Howard, J.C., Beer, S., Pfeffer, K., Coers, J., and Taylor, G.A. (2011). Immunity-related GTPase M (IRGM) proteins influence the localization of guanylate-binding protein 2 (GBP2) by modulating macroautophagy. J Biol Chem 286, 30471-30480.

Weisberg, S.P., McCann, D., Desai, M., Rosenbaum, M., Leibel, R.L., and Ferrante, A.W. (2003). Obesity is associated with macrophage accumulation in adipose tissue. J Clin Invest 112, 1796-1808.

Weiss, E.C., Galuska, D.A., Kettel Khan, L., Gillespie, C., and Serdula, M.K. (2007). Weight regain in U.S. adults who

experienced substantial weight loss, 1999-2002. Am J Prev Med 33, 34-40.

Wensveen, F.M., Jelencic, V., Valentic, S., Sestan, M., Wensveen, T.T., Theurich, S., Glasner, A., Mendrila, D., Stimac, D., Wunderlich, F.T., Bruning, J.C., Mandelboim, O., and Polic, B. (2015). NK cells link obesity-induced adipose stress to inflammation and insulin resistance. Nat Immunol 16, 376-385.

Winer, D.A., Winer, S., Shen, L., Wadia, P.P., Yantha, J., Paltser, G., Tsui, H., Wu, P., Davidson, M.G., Alonso, M.N., Leong, H.X., Glassford, A., Caimol, M., Kenkel, J.A., Tedder, T.F., McLaughlin, T., Miklos, D.B., Dosch, H.M., and Engleman, E.G. (2011). B cells promote insulin resistance through modulation of T cells and production of pathogenic IgG antibodies. Nat Med 17, 610-617.

Winer, S., Chan, Y., Paltser, G., Truong, D., Tsui, H., Bahrami, J., Dorfman, R., Wang, Y., Zielenski, J., Mastronardi, F., Maezawa, Y., Drucker, D.J., Engleman, E., Winer, D., and Dosch, H.M. (2009). Normalization of obesity-associated insulin resistance through immunotherapy. Nat Med 15, 921-929.

Wing, R.R., and Hiil, J.O. (2001). Successful weight loss maintenance. Annu Rev Nutr 21, 323-341.

Wu, H., Ghosh, S., Perrard, X.D., Feng, L., Garcia, G.E., Perrard, J.L., Sweeney, J.F., Peterson, L.E., Chan, L., Smith, C.W., and Ballatyne, C.M. (2007). T-cell accumulation and regulated on

activation, normal T cell expressed and secreted upregulation in adipose tissue in obesity. Circulation 115, 1029-1038.

Xu, H., Barnes, G.T., Yang, Q., Tan, G., Yang, D., Chou, C.J., Sole, J., Nichols, A., Ross, J.S., Tartaglia, L.A., and Chen, H. (2003). Chronic inflammation in fat plays a crucial role in the development of obesity-related insulin resistance. J Clin Invest 112, 1821-1830.

Yang, H., Youm, Y.H., Vandanmagsar, B., Ravussin, A., Gimble, J.M., Greenway, F., Stephens, J.M., Mynatt, R.L., and Dixit, V.D. (2010). Obesity increases the production of proinflammatory mediators from adipose tissue T cells and compromises TCR repertoire diversity: implications for systemic inflammation and insulin resistance. J Immunol 185, 1836-1845.

국문초록

비만은 제 2형 당뇨병, 심혈관계 질환과 같은 대사 질환과 밀접한 관련이 있으며, 비만을 완화하기 위한 이상적인 방법으로는 체중감량이 있다. 하지만 체중감량은 그 상태를 유지하기 힘들며 체중의 재 증가로 이어진다. 이러한 체중의 감량, 체중의 재 증가 현상을 중량 사이클링이라고 하며, 요요현상으로 잘 알려져 있다. 중량 사이클링은 사람과 마우스에서 질병 및 사망률을 증가시킨다고 알려져 있는 반면 중량 사이클링을 조절 할 수 있는 방법은 현재까지 명확히 밝혀지지 않았다. 따라서 본 연구에서는 식이섭취의 기간과 종류를 변화시키는 마우스 사육계획을 통해 중량 사이클링으로 비만을 유도하고 대조군과의 차이점을 규명하였다.

중량 사이클링을 마우스에 적용하기 위해 마우스의 식이섭취 사육은 “체중 증가 - 체중감소 - 체중의 재 증가“의 세 번의 기간을 포함하였다. 첫 번째 기간에는 고지방식이의 섭취를 통해 마우스에 비만을 유도하여 체중을 증가 시켰고, 일반식이로의 식이섭취 전환으로 두 번째 기간의 대조군과 유사한 수준으로 체중을 감소시킨다. 마지막 기간에 다시 고지방식이를 섭취하게 하여 체중의 재 증가를 유도하였다.

중량 사이클링 그룹은 체중, 간과 지방조직의 중량이 증가되었으며 혈액 대사 파라미터와 같은 비만과 관련된 표현형이 더 심각하게 나타났다. 중량 사이클링 그룹의 간 조직에서는 간지방증이 증가했으며 지질의 이상축적이 관찰되었다. 중량 사이클링 그룹의 지방조직에서는 비대한 지방세포가 증가했으며 왕관 유사구조 지방세포의 증가로 인해 면역반응이 증가했음을 관찰했다. 면역학적 조직염색을 통해 증가된 왕관 유사구조 지방세포의 면역세포가 M1 대식세포임을 확인했다. 지방세포에서 면역세포, 특히 M1 대식세포의 침윤 증가는 지방세포가 전 염증상태로 변화된 것을 의미한다. 이와 관련해

서, 중량 사이클링 그룹의 지방조직에서 면역 관련 유전자와 전 염증성 사이토카인 유전자의 발현이 증가한 것을 확인하였다. 또한 지방조직에서 면역반응과 관련된 유전자 발현이 중량 사이클링 그룹과 비만 마우스의 지방세포, 기질 혈관 분획에 속한 세포에서 증가되는 것을 확인하였다. 따라서 중량 사이클링 동안에 지방세포에서 면역세포 구성의 변화와 면역 관련 유전자 발현의 변화가 비정상적인 대사표현형과 관련이 있음을 알 수 있다.

주요어 : 비만, 중량 사이클링, 마우스, 지방 조직, 염증.
학번 : 2013-23443